Aerosol and Air Quality Research, 16: 1427–1440, 2016

ISSN: 1680-8584 print / 2071-1409 online
doi: 10.4209/aaqr.2014.09.0220

Characterisation of Absorbing Aerosols Using Ground and Satellite Data at an Urban Location, Hyderabad

Subin Jose[1], Kaundala Niranjan[2], Biswadip Gharai[1*], Pamaraju Venkata Narasimha Rao[1], Vijayakumar S. Nair[3]

[1] *Atmospheric & Climate Sciences Group, ECSA, NRSC, Balanagar, Hyderabad, India*
[2] *Department of Physics, Andhra University, Andhra Pradesh, India*
[3] *Space Physics Laboratory (SPL), Vikram Sarabhai Space Centre, Trivandrum, India*

ABSTRACT

In the present study we have attempted to characterize aerosols using their optical properties over a tropical urban location of Hyderabad, India. We have analyzed three years of in-situ data on aerosol absorption from Aethalometer and scattering from Nephelometer measurements. Satellite based absorption measurements from ozone monitoring instrument, absorbing aerosol index are also analyzed to investigate the role of long range transport of dust. Further, the Cloud–Aerosol Lidar Pathfinder Satellite Observations (CALIPSO) data is used to study the vertical extent of aerosol particles as well as their sphericity using its particulate depolarization ratio. The study revealed that irrespective of seasonal variation, local anthropogenic fossil fuel aerosols form the predominant aerosol type over this site. Biomass/dust aerosols in their pure form are not present during the study period; however the spread of frequency distribution of scattering Angstrom exponent and absorption Angstrom exponent suggested their possible existence in mixed condition with local anthropogenic aerosols. The analysis of columnar aerosol absorption data during pre-monsoon period showed the dominance of UV absorbing dust aerosols in the study region. CALIPSO data analysis over study area showed that majority aerosols are confined within 2 km from the surface during winter while in pre-monsoon particles are distributed throughout the profile (~6 km) with extinction coefficient varying between 0.1–0.2 km^{-1}. As the season shift from winter to pre-monsoon a change in sphericity of particle is observed. Cluster mean trajectory analysis revealed that during pre-monsoon majority of air mass movements (~68%) are from western side passing through dust source region like Persian Gulf and Thar Desert before entering into Indian region. During post-monsoon (~70%) and winter (~65%), majority of the air masses are coming from north-west and north-east side of the study area where biomass burning is quite frequent during this period.

Keywords: Absorption coefficient; Angstrom exponent; Black carbon; Aerosol index and particulate depolarization ratio.

INTRODUCTION

Aerosols represent unique particulate constituents that have significant impact on climate (Myhre *et al.*, 2013). Depending upon their intrinsic and extrinsic properties, they perturb the radiation balance directly through scattering and absorbing solar radiation (Ardanuy *et al.*, 1992; Haywood and Shine, 1995) and indirectly by affecting the optical properties and lifetimes of clouds (Rosenfeld, 1999, 2000). Over the last decade there has been a tremendous progress in the understanding of aerosol causing climatic effects with some important observational and modelling breakthroughs (Takemura *et al.*, 2005; Putaud *et al.*, 2010; Andrews *et al.*, 2011). However, still there exist great uncertainties associated with their radiative effect because of the greater complexity in emission sources and formation mechanism (Penner *et al.*, 1994) and hence in quantification of their climate effect.

Majority of the known aerosol types like sulphates, organics, mineral dust, sea salt etc. scatter incoming solar radiation and thereby reduce the energy flux reaching the Earth's surface, thus cooling the earth surface (Charlson *et al.*, 1991). These scattering aerosols counteract the warming effects induced by anthropogenic greenhouse gases by an uncertain, but potentially large amount (Andreae *et al.*, 2005). But there are some aerosols where their absorbing component dominates their scattering part; soot or Black Carbon (BC) which is produced as a result of incomplete combustion is an example for this kind. BC is considered as an important benchmark to determine the air quality of a

* Corresponding author.
Tel.: +9104023884467
E-mail address: g.biswadip@gmail.com

region and has increased many folds in the developing countries due to rapid urbanisation and development (Streets *et al.*, 2001). Hence, in recent years scientific attention has focused largely on the role of these anthropogenic aerosols in climate change (Andreae, 1995; Hansen *et al.*, 1998, 2005). It is considered to be the second largest contributor to global warming after carbon dioxide (Ramanathan and Carmichael, 2008; Jacobson, 2010) and recent studies have revealed that total estimated climate forcing of BC is about +1.1 W m^{-2} (Bond *et al.*, 2013) approximately two thirds of the effect of CO_2. Fresh Soot is normally hydrophobic and therefore acts as poor Cloud Condensation Nuclei (CCN) and its absorption coefficients shows weak spectral dependence in the solar spectrum (Bergstrom *et al.*, 2002; Kirchstetter *et al.*, 2004). Bond and Bergstrom (2006) have calculated the mass absorption efficiency for fresh soot aggregates at 550 nm to be 7.15 ± 1.2 m^2 g^{-1}. Another important anthropogenic absorbing aerosol that has great climatic relevance and not well addressed in climate model is Brown Carbon (Andreae and Gelencsér, 2006). It is usually formed by inefficient combustion of hydrocarbons (e.g., smoldering) (Patterson and McMahon, 1984) or from industrial combustion of lignite. Absorption coefficient of these particles show strong spectral dependence and have less mass absorption efficiency compared to soot (Kirchstetter *et al.*, 2004; Hoffer *et al.*, 2006; Clarke *et al.*, 2007). Mineral aerosol which is either from long range transport or local resuspension also significantly absorbs solar radiation. The presence of ferric iron oxides such as hematite and goethite in dust aerosols can significantly increase the absorption in the UV/ Visible region of solar spectrum and hence show a strong spectral dependence of absorption coefficient (Sokolik and Toon, 1999). On a regional scale the forcing due to mineral aerosols can greatly exceed that due to sulphate aerosols and can be comparable to that of clouds (Sokolik and Toon, 1996). The reported values of mass absorption efficiencies of dust aerosol from Gobi (China), Sahara (Tunisia) and Sahel (Nigeria) range from 0.01–0.02 m^2 g^{-1} at 660 nm (Alfaro *et al.*, 2004). In addition to these absorbing aerosols, mixing of optically and chemically different aerosols also plays important role in absorption of solar radiation. For instance sulphate coated with black carbon absorbs more radiation than a pure black carbon (Schwarz *et al.*, 2008). Fuller *et al.* (1999) have shown that a complete encapsulation of a soot core with a non absorbing organic or inorganic condensates might enhance the absorption by 30–50%.

In India, there has been a substantial increase in aerosol emission during the last decades due to rapid urbanisation and population growth (Menon *et al.*, 2002). Venkatraman *et al.* (2005) have showed that in India ~44% of BC emission comes from bio fuel combustion. Biomass burning which includes agriculture residue burning and forest fire are quite common during dry seasons (Sharma *et al.*, 2010). Dust storms originating from Persian Gulf and Thar desert regions are also quiet frequent over this region during pre-monsoon (Gharai *et al.*, 2013). Moorthy *et al.* (2007) have inferred that dust aerosols from 'Great Indian Desert' are more absorbing in nature than dust aerosols from African desert. These absorbing aerosols exert a positive radiative forcing at top of the atmosphere causing a warming effect to climate system and hence cause surface cooling (Penner *et al.*, 1994). It also influences atmospheric thermal stability, surface heat exchange, evapotranspiration, and also air circulation as well as formation and development of clouds.

In the present study we investigated the presence of absorbing aerosols in a tropical urban location, Hyderabad, India. Towards this, ground based observations from Aethalometer and satellite based observation from Ozone Monitoring Instrument (OMI) are analysed. Scattering component from the unloaded filter tape of Aethalometer is addressed by incorporating simultaneous observations of scattering, by Nephelometer. The vertical extent of aerosol is studied using CALIPSO data, and potential source locations are identified using cluster mean trajectory analysis.

EXPERIMENTAL SITE, DATA AND METHODOLOGY

The present study is conducted at Hyderabad, a tropical urban site in the campus of National Remote Sensing Centre (NRSC) (17.47°N, 78.43°E). Hyderabad is the capital of the newly formed state Telangana, with a population of more than 4 million (http://censusindia.gov.in). The study site is situated on the Deccan plateau at a height of 557 m above mean sea level. It has a hot semi-arid steppe climate with four dominant seasons; winter (Dec–Jan–Feb), pre-monsoon (Mar–Apr–May), monsoon (Jun–Jul–Aug–Sep) and post-monsoon (Oct–Nov). The meteorological parameters recorded at India Meteorological Department (IMD) (www.imd.gov.in), Begumpet, Hyderabad over a period of 1997–2012 was analysed. Study revealed that long term daily mean of maximum (T_{max} = 36.1°C) and minimum temperatures (T_{min} = 17.54°C) are similar to that was observed during the study period of 2010-2012 (T_{max} = 36.0°C and T_{min} = 17.33°C). However, analysis of diurnal variation of temperature recorded during study period of 2010–2012 shows that T_{max} and T_{min} are ~42°C and ~16°C, respectively. The long term (1997–2012) mean relative humidity varies between 40–80% with lowest observed during premonsoon and maximum during monsoon. The local wind speed varies typically from 5–15 m s^{-1}, with a maximum observed during monsoon. The long term (1957–2012) annual mean of rainfall over Hyderabad is ~827 mm, while the annual rainfall over Hyderabad during the study period 2010–2012 is found to be 1192 mm, 625 mm and 778 mm, respectively. The sampling site is near the state high way and the main sources of aerosols are from vehicular emission, local/long range transport of dust aerosols, biomass burning and industrial emissions.

Ground Based Observation

Black Carbon Measurement

Absorbing aerosol measurements are carried out using a seven channel (370 nm, 470 nm, 520 nm, 590 nm, 660 nm, 880 nm and 950 nm) Aethalometer (model AE31, Magee Scientific, USA). It works on the principle of optical attenuation by aerosol particles deposited on a quartz fibre tape. Attenuation at 880 nm is considered as the standard for

calculating Black Carbon (BC) mass concentration as there is no other major aerosol species which shows significant absorption at this wavelength. The attenuation of light is converted to the recorded BC mass concentration using wavelength dependent calibration factors as recommended by the manufacturer (Aethalometer Manual, Magee Scientific, USA). It is operated at a flow rate of 3 L min^{-1} (lpm) with a data averaging time of 5 min. More details about the instrumentations and the calibration factors used for calculating mass concentrations can be obtained from Hansen *et al.* (1984, 1996). In the present study, three years (2010–2012) of BC data are analyzed. BC mass concentration is diurnally averaged after screening out those data points above and below mean ± 3σ (standard deviation), for the purpose of outlier filtering (Blalock, 1960) and thereby maintaining the data quality. During 3σ screening every hourly data is considered as individual bin. Further, data sets are created by taking the mean value of respective days during the entire study period and are used for further analysis.

Scattering Coefficient

Scattering coefficient of suspended particulate matter during the study period is measured using an integrating Nephelometer (TSI- 3653, USA). It measures total scattering (σ_{sca}) and hemispheric backscattering (σ_{bsca}) at three wavelengths (450 nm, 550 nm and 700 nm). Instrument is operated at flow rate of 20 L min^{-1} and with a time resolution of 5 min. Details of instrumentation, operational principle and calibration procedures are available in Anderson *et al.* (1996). Instrument was calibrated regularly during the study period using CO_2 and air as high span and low span gases, respectively. The measured data are corrected for angular truncation error and for non ideality in the geometry of the instrument following the method suggested by Anderson and Ogren (1998). The uncertainty range associated with angular truncation error of σ_{sca} is in the range of –3% to +5% (Heintenberg and Bhardwaja., 1976). Spectral dependence of σ_{sca} is sensitive to particle size and can be qualitatively expressed in terms of Scattering Angstrom Exponent (SAE). This parameter depends primarily on the particles' size and ranges from 4 (Rayleigh atmosphere) to 0 (large particles) (Valenzuela *et al.*, 2015).

Aerosol Absorption Coefficient (σ_{abs}) Calculation

The multi-spectral raw Aethalometer data is suffered by two factors viz. (1) in a nearly unloaded condition, fiber filter causes multiple scattering, which in turn enhanced the light absorption and (2) decrease in optical path length within Aethalometer filter tape due to enhanced filter loading (shadowing effect) causing underestimating the measured signal (Weingartner *et al.*, 2003). In the present study we calculated absorption coefficient of aerosols at different wavelength by using a two stream radiative transfer model proposed by Arnott *et al.* (2005). Scattering offset associated with determination of σ_{abs} is taken care by using simultaneous measurement of wavelength-dependent scattering measured from a 3-wavelength Nephelometer. Multiple scattering theory is used to analytically obtain a filter-loading correction function. The corrected σ_{abs} is given by

$$\sigma_{abs,n} = \frac{\sigma_{ATN,n} - \alpha \times \sigma_{SCA,n}}{C_{ref} . R_{A,n}} \quad (1)$$

where σ_{ATN} is the raw absorption coefficien, σ_{SCA} is the scattering coefficient and Ra is the Arnott filter-loading correction term at time n. The necessary correction factors required for calculation of σ_{abs} are adopted from Arontt *et al.* (2005). Compare to other models, the methodology suggested by Arontt *et al.* (2005) has a better theoretical footing, even though it is more complicated. The expected uncertainties in the estimation of σ_{abs} using this methodology are generally less than 10%. In general, the spectral dependence of aerosol absorption coefficients follows power law relationship

$$\sigma_{abs}(\lambda) = k\lambda^{-AAE} \quad (2)$$

where $\sigma_{abs}(\lambda)$ is the aerosol absorption coefficient at wavelength λ; k a constant and AAE is the Absorption Angstrom Exponent as discussed by Kirchstetter *et al.* (2004). We calculated AAE by taking the negative slope of absorptions vs. wavelengths (370 nm–950 nm) in a log-log plot. The value of AAE can be used to discriminate between different carbonaceous aerosols, as several studies have found that aerosols originating from fossil fuel combustion show weaker dependence on spectral light absorption, with AAE value close to 1 and AAE values between 1 and 2 are an indicator of mixture of BC origin from fossil and biomass fuel (Kirchstetter *et al.*, 2004; Bergstrom *et al.*, 2007).

Satellite Based Observations

Ozone Monitoring Instrument (OMI)

The retrieval of aerosol absorption properties from space is still one of the challenging areas in satellite remote sensing. However the concept of Aerosol Index (AI) for the detection of absorbing aerosols in UV region based on Total Ozone Mapping Spectrometer (TOMS) observations is still a reliable estimate in the respective spectral domain (Herman *et al.*, 1997; Torres *et al.*, 1998). In the present study level 3 AI data obtained via OMI/AURA Level 3 Total column ozone data product OMTO3d (version 003) which is available from the NASA Goddard Earth Sciences Data and Information Services Center (http://mirador.gsfc.nasa.gov/) is used for the analysis. The AI used in the OMI aerosol algorithm is defined as

$$AI = 100[\log_{10}(I_{360}/I_{331})_{meas} - (\log_{10}(I_{360}/I_{331})_{calc}] \quad (3)$$

where the indices "*meas*" and "*calc*" indicate the radiance measured by OMI and the radiance calculated for pure Rayleigh scattering, respectively (Torres *et al.*, 1998). Because of the short separation of the wavelengths involved, the surface effect in the computation of the UV aerosol index is very small. When UV absorbing aerosols are present in the atmosphere, the spectral contrast (I_{360}/I_{331}) is smaller than that predicted by the calculation model, and positive residues are produced by Eq. (3). Non- absorbing aerosols produce greater spectral contrast, and thus result in negative AI. Near zero values of AI indicate presence of cloud. Since AI is

dependent on aerosol concentration, optical properties and altitude of the aerosol layer, complementary observations of AOD from Moderate Resolution Imaging Spectro radiometer (MODIS) in aqua platform and attenuated backscatter coefficients from the Cloud-Aerosol Lidar and Infrared Pathfinder Satellite Observation (CALIPSO) are used.

Moderate Resolution Imaging Spectroradiometer (MODIS)

MODIS has 36 spectral bands ranging from 0.4 to 14.4 μm with three different spatial resolutions (250 m, 500 m and 1000 m). It has a swath of 2330 km and provides near global coverage on daily scale with an equatorial crossing local time of 10.30 and 1.30 for Terra and Aqua platform, respectively. In this study we have used Level 3 AOD_{550nm} data from Aqua platform, which is available from (https://ladsweb.nascom.nasa.gov/). The expected uncertainty of MODIS AOD retrieval over land is observed to be ± 0.05 ± 0.15 AOD (Remer *et al.*, 2008).

Cloud Aerosol Lidar and Infrared Path Finder Satellite Observation (CALIPSO)

CALIPSO is a joint NASA-CNES mission, launched on 28 April 2006 in a sun synchronized orbit at an altitude of 705 km from the earth. CALIOP (Cloud Aerosol Lidar and Infrared Path finder), which is one of the primary instruments on the satellite providing vertical profiles of atmospheric aerosols at two wavelengths (1064 nm and 532 nm) from a near nadir-viewing geometry during both day and night phases of the orbit. In addition to the back scatter vertical profiles at two wavelengths it also provides profiles of particle depolarization ratio (PDR) at 532 nm. The depolarization measurement enables the discrimination between ice clouds and water and non-spherical aerosol particles (Huang *et al.*, 2007). In the present study we used CALIPSO Level 2 data, version 3.02 during 2006–2012, obtained from NASA site (http://www-calipso.larc.nasa.gov/). The dataset for pre-monsoon and winter consist of 59 and 63 CALIPSO tracks, respectively. The tracks during night time only are used in the analysis as it is more sensitive than those during day time (Zwally *et al.*, 2002). The mean extinction and depolarization ratio profiles over Hyderabad region are analysed. Basic quality screening technique, Atmospheric Volume Description (AVD) is used to remove false features like cloud layer from the profile, further aerosol layer having a Cloud Aerosol Discrimination (CAD) score greater than –20 have been screened out and also outputs are further screened depending on their respective uncertainty values (Yang *et al.*, 2012).

CALIPSO is the only satellite currently in orbit which provides three dimensional distributions of aerosol properties with certain uncertainties. These are (1) the large distances between the lidar and the target of interest (typically between 500 km–700 km), (2) the high speed at which laser sweeps across the target space (~7 km s^{-1}) and (3) the relatively low firing rate of the laser (20Hz) relative to the velocity of satellite (Winker *et al.*, 1996).

HYbrid Single Particle Lagrangian Integrated Trajectory (HYSPLIT) Model

The general air mass pathway reaching Hyderabad is analysed using HYSPLIT model (Draxler and Rolph, 2003) [http://ww.arl.noaa.gov/ready/hysplit4.html]. We computed 5 day isentropic model backward air mass trajectory for all days from 2010–2012 with each trajectory starting at 00:00 hrs and reaching study site, Hyderabad at two levels,1000 and 3000 m above ground level (AGL). Even though the trajectory analysis have inherent uncertainties (Stohl, 1998), they are quite useful in determining pollutants pathways.

RESULTS AND DISCUSSION

BC Variability

Diurnal variation of BC averaged for the study period is shown in Fig. 1(a) (Top panel). A well-defined diurnal variation is observed in all seasons with two peaks during morning 07:00–09:00 local time (LT) and night 20:00 LT onwards also with an afternoon minimum (11:00–17:00 LT). A similar diurnal pattern of BC is also observed in other parts of the country (Babu *et al.*, 2002; Beegum *et al.*, 2009). The diurnal variation of BC is highly influenced by the diurnal evolution of atmospheric boundary layer (ABL) and its structure (Moorthy *et al.*, 2003; Nair *et al.*, 2007). The mechanism for morning peak is closely associated with the fumigation effect (Nair *et al.*, 2007), where BC in the residual layer mixes with the surface layer by mixed layer entrainment and turbulence in addition to building up of anthropogenic activities (mostly vehicular emissions and industrial emissions) (Stull, 1998). As the day progress due to surface heating, atmospheric aerosols near surface get diluted in their concentration and push the ABL upwards resulting in less concentration of BC during the day time. In addition, low traffic density compared to morning and evening peak traffic movements are also one of the causes of lower concentration of BC observed during day time. During evening time, solar heating decreases and hence atmospheric convective activity also decreases, which inhibits the vertical transport of aerosols resulting in a nocturnal peak as seen in the figure.

Monthly mean variation of BC mass concentration (μg m^{-3}) in box plot is shown in Fig. 1(b) (Bottom Panel). The range of box represents the values between 25–75 percentiles, the wisker represent standard deviation, minimum and maximum values are represented by asterisk, mean and median values are described by square and straight line inside the box. BC mean (± standard deviation) mass concentration during pre-monsoon, monsoon, post-monsoon and winter is found to be 13.16 ± 2.62, 11.66 ± 1.81, 14.84 ± 1.37, 13.12 ± 2.42 μg m^{-3} respectively. There is a seasonal difference in BC mass concentration with low values during monsoon and higher values during the rest of the seasons. Though the BC particles are not hygroscopic, rainfall can contribute to reduction of BC particles by wet scavenging and by increasing the probability of condensation of secondary inorganic aerosols on BC particle which can make them hygroscopic and get scavenged by precipitation due to the presence of high humidity prevailing during these months (Gadhavi and Jayaraman, 2010). The BC mean mass concentration observed a maximum [~15.91 μg m^{-3}] during the month of March and a minimum in June [~9.84 μg m^{-3}].

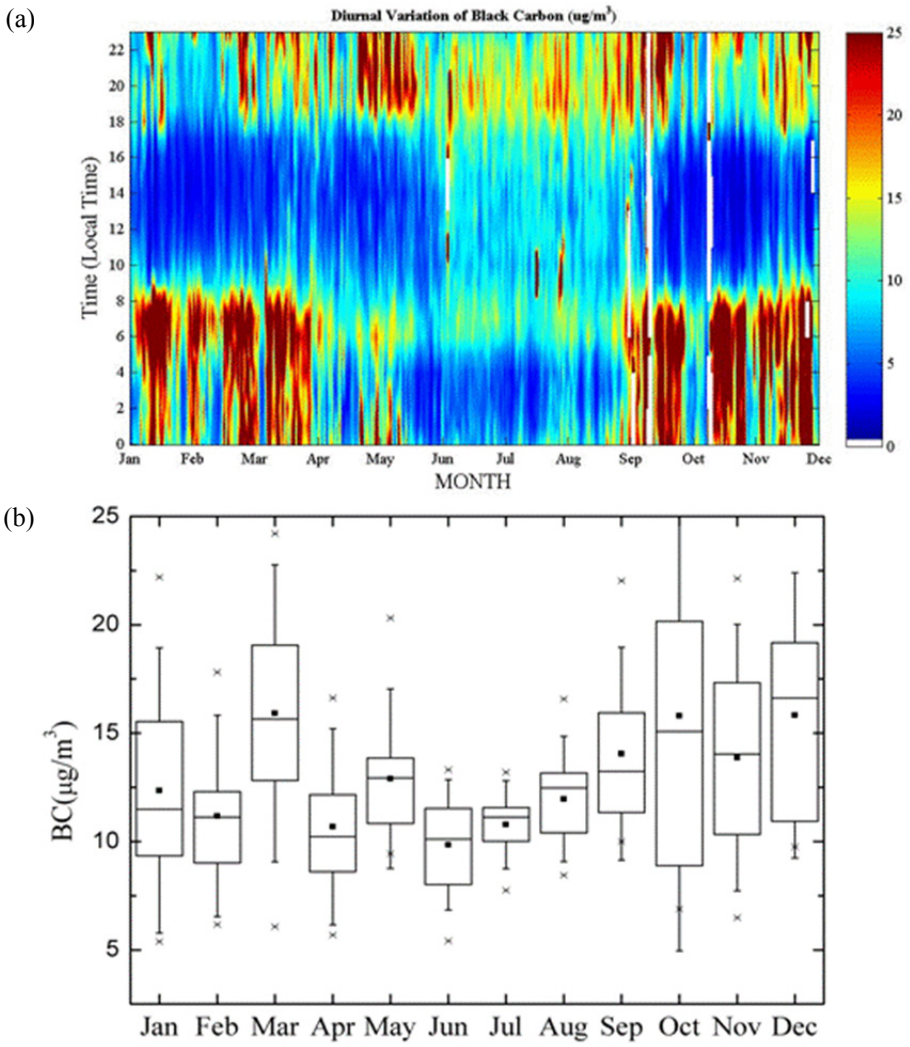

Fig. 1. Temporal variation of Black Carbon at the surface in Hyderabad during 2010–2012: (a) mean diurnal variation of BC; (b) monthly box plot variation of BC.

A gradual increase of BC mean mass concentration can also be observed from June to December [~15.82 µg m^{-3}]. These seasonal variations can be attributed to dynamics of monsoon circulation, ABL characteristics (Moorthy *et al.*, 2003; Nair *et al.*, 2007) and the prevailing meteorological conditions.

The BC mass concentration reported from other urban sites of the country like Delhi [3–27 µg m^{-3}] (Beegum *et al.*, 2009), Ahemdabad [0.2–10.2 µg m^{-3}] (Ramachandran and Rajesh, 2007), Mumbai [12.4 ± 5.1 µg m^{-3}] (Venkatraman *et al.*, 2002), Kanpur [6–20 µg m^{-3}] (Tripathi *et al.*, 2005) and Bangalore [0.4–10.2 µg m^{-3}] (Babu *et al.*, 2002) is quite comparable to those observed over Hyderabad [9–16 µg m^{-3}] during the study period. The frequency distribution of BC daily mean mass concentration during the study period (not shown here) shows that ~63% of study days, BC values are between 5–15 µg m^{-3}, while only ~6% of the days BC values are less than 5 µg m^{-3}.

Aerosol Absorption and Scattering Coefficient

Although BC mass concentration is an important parameter in assessing the air quality of a region, the radiative impact of the aerosols can be studied only if the absorption coefficients (σ_{abs}) and scattering coefficients (σ_{sca}) of these aerosols are known. It is a necessary input for the calculation of Single Scattering Albedo (ω), which is one of the critical parameters in aerosol radiative forcing calculation (Hansen *et al.*, 1998). The observed values of mean σ_{abs} (550 nm) and σ_{sca} during different seasons over Hyderabad and the reported values in other cities are shown in Table 1. The mean σ_{sca} (Mm^{-1}) over Hyderabad during pre-monsoon, post-monsoon and winter are 170 ± 55, 181 ± 20.4, 298 ± 57 Mm^{-1} respectively, while mean σ_{abs} (Mm^{-1}) during same period are 81 ± 38.03, 56 ± 47.37, 84 ± 35.85 Mm^{-1} respectively.

Apart from radiative forcing studies, the information from the wavelength dependence of σ_{abs} (quantitatively through AAE) and σ_{sae} (quantitatively through SAE) can be used for aerosol species identification (Fialho *et al.*, 2005). Several studies have found that aerosols originating from fossil fuel combustion show weaker dependence on spectral light absorption while the biomass burning aerosols and dust

Table 1. Aerosol absorption coefficient observed in different cities.

City	Lat Long	Period	σ_{abs} ± stdev (Mm^{-1})	σ_{sca} ± stdev (Mm^{-1})	Reference
Delhi	28°36'N 77°12'E	**2008–2009** Summer Winter Spring	 62 ± 21 (550 nm) 189 ± 86 90 ± 33	 110 ± 36 (550 nm) 566 ± 274 236 ± 96	Soni *et al.*, 2010
Hyderabad	17.47°N, 78.43°E	**2010–2012** Pre-monsoon Winter Post-monsoon	 81 ± 38 (550 nm) 56 ± 47 84 ± 35	 170 ± 55 (550 nm) 181 ± 20.4 298 ± 57	Present study
Ahmedabad	23°1'N 72°34'E	**2002–2005** Summer Winter Post-Monsoon	 ~48(520 nm) ~98 ~104	 ~150 (530 nm) ~205 ~310	Ganguly *et al.*, 2006
Kanpur	26.5°N, 80.3° E	Jan 2007–Feb 2008	22–236 Mm^{-1}	-	Ram *et al.*, 2010
Vishakaptnam	17.72°N, 83.32°E	2007	~20–110 Mm^{-1} (550 nm)	~50–450 Mm^{-1} (550 nm)	Niranjan *et al.*, 2011
La Merced Mexico	29°94'N 107°53'W	1997.02–28– 1997.03–10	80.8 ± 32 (880 nm)	225 ± 132	Silvia, 2002
Lin'an	30°14'N 119°43'E	**2004** Spring	44.3 ± 19.7 (532 nm)	229 ± 104	Yan., 2006
Beijing	39°54'N 116°24'E	**2005 & 2006** Spring Summer Winter	 45 ± 39 (532 nm) 54 ± 40 58 ± 57	 243 ± 255 351 ± 294 259 ± 284	He *et al.*, 2009
Wuqing	39°23'N 117°2'E	**2009** Spring	47 ± 38 (637 nm)	280 ± 253	Ma *et al.*, 2011

aerosols show a stronger spectral dependence (Bergstorm *et al.*, 2002; Krischestter *et al.*, 2004). In the present study we tried to investigate the probable presence of different aerosol types by analyzing their spectral dependence on absorption and scattering coefficient. The seasonal variations of spectral scattering coefficient (σ_{sca}) and spectral absorption coefficient (σ_{abs}) are depicted in Fig. 2(a). Analysis shows that seasonal average SAE values during pre-monsoon, post-monsoon and winter are 1.56 ± 0.27, 1.5 ± 0.18 and 1.63 ± 0.11 respectively, where as respective AAE values are 1.19 ± 0.16, 1.2 ± 0.18 and 1.2 ± 0.16. This clearly indicates the dominance of fossil fuel aerosols in these seasons, which is as expected in an urban site like Hyderabad; however the presence of long range transported aerosols can't be rule out. During post-monsoon and winter season biomass burning activities (which include forest fire and agriculture residue burning) are quite prominent over the Indian regions (Rastogi and Sarin, 2005); also frequency of dust storm and the presence of local resuspended soil dust aerosols is more during the pre-monsoon months. Moorthy *et al.* (2007) have inferred that dust aerosols over the Great Indian Desert (which is in the NW side of study site) is more absorbing in nature compared to other African desert dust aerosols. Kaskoutis *et al.* (2009) have reported a ~2 fold increase in aerosol optical depth (AOD) during an intense dust storm over Hyderabad during pre-monsoon of 2008, while Kharol and Badrinath (2006) have suggested a reduction –12.5 W m^{-2} of broad band radiation per 0.1 increase in AOD due to the presence of biomass burning aerosols. During their life time, these aerosol can also adhere with local anthropogenic aerosols (BC) forming a complex aerosol type with different physical, optical and chemical properties (Fuller *et al.*, 1999; Jacobson, 2001; Bond and Bergstorm, 2006). AAE depends on the wavelength pair as well as the mixing and coating state of the aerosols. Gyawali *et al.* (2012) found AAE close to one during clean days and with little variation but around 0.8 during polluted days, with a wavelength pair 532/870 nm. The value of AAE < 1 can be related to black carbon coating by coarse particles such as dust and organic carbon (Giles *et al.*, 2010). Over Kanpur, India, Eck *et al.* (2010) found AAE (440–870 nm) approaches 2 for coarse dust. Kirchstetter *et al.* (2004) has reported an average AAE value of 1.2 for biomass burning aerosol haze samples collected during SAFARI 2000. In-order to investigate the probable presence of biomass/dust aerosols during different season, frequency distributions of SAE and AAE are analyzed, and is shown in Figs. 2(b), 2(c) and 2(d). The predominance of fossil fuel aerosol during all the seasons is underlined by the presence of majority of AAE values falling within the range 1.1–1.3 and SAE values 1.3–1.7. A closer observation of Figs. 2(b), 2(c) and 2(d) shows that during post-monsoon and winter season ~16–25% of the total AAE values are greater than 1.5, while this is ~10% in pre-monsoon; AAE values below 0.9 during pre-monsoon, post-monsoon and winter are respectively ~11%, ~23% and ~8%. Presence of coarse mode aerosol (probably

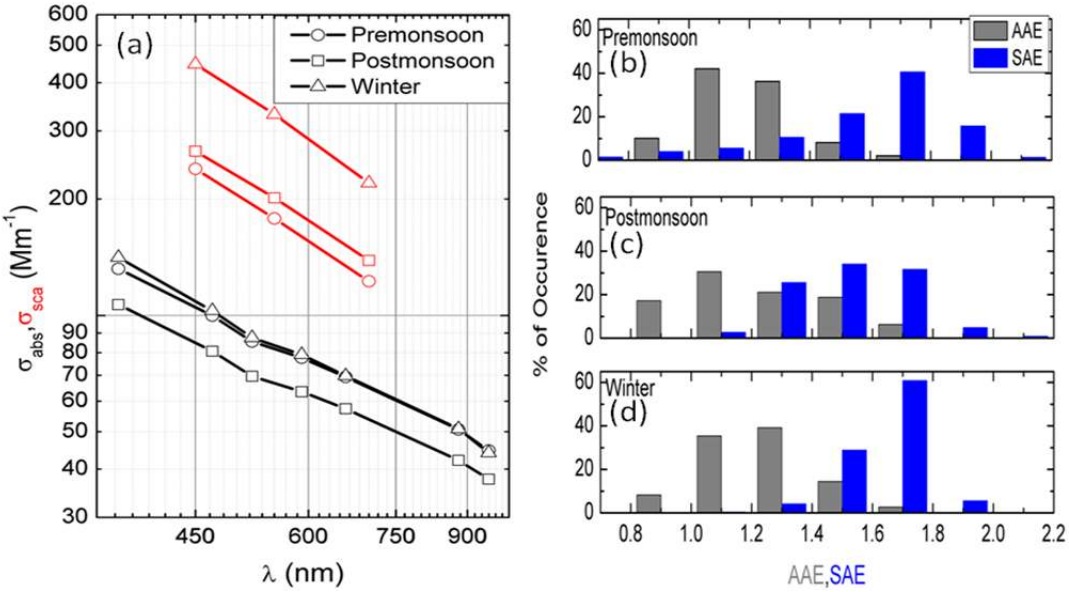

Fig. 2. (a) Seasonal variation of absorption coefficient (σ_{abs}) and scattering coefficient (σ_{sca}); Frequency distribution of AAE and SAE during (b) pre-monsoon, (c) post-monsoon and (d) winter over Hyderabad during 2010–2012.

dust) with low SAE values can be observed during pre-monsoon. Although seasonal differences in frequency of AAE and SAE values are not significant, this variation can be attributed to the presence of other aerosols like organic carbon (from biomass burning), dust etc. in different relative amounts coated with local anthropogenic aerosols either internally or externally (Sandradevi *et al.*, 2008; Giles *et al.*, 2010).

The frequency distribution of SAE and AAE during study period reveals that predominant aerosol type over Hyderabad is from local fossil fuel aerosols. The presence of biomass burning aerosols or dust aerosols in its pure form are not prominent during study period at the surface; however spread of frequency spectrum of SAE and AAE possibly suggest the presence of these aerosols types in mixed form with local anthropogenic aerosols. Further laboratory studies under controlled environment are required to confirm their nature of existence with BC and hence to determine the absorption efficiency of these complex mixtures.

Satellite Observations

Aerosol Index (AI) provided by OMI gives a global as well as regional columnar measurement of aerosol absorption. It is an effective index to characterize UV absorbing aerosols like dust, smoke, volcanic ash from non-absorbing ones (Torres *et al.*, 1998). One of the main drawbacks of AI retrieved by OMI is, it is sensitive to aerosol layer height and any aerosol below 1000 m is unlikely to be detected or yield negative values since weakly absorbing aerosols at low altitudes cannot be distinguished from non-absorbing aerosols (Torres *et al.*, 1998; De Graaf *et al.*, 2005). In the present study, Aerosol Index data are analyzed independently to investigate on long range transport of absorbing aerosols e.g., dust. Since aerosols below 1000 m are not properly represented by OMI derived AI, ground based Aethalometer measurements are not directly analyzed in conjunction with AI. Here we tried to analyze the long term variation of AI over Hyderabad; the box plot of monthly mean variation of AI during 2006–2012 is shown in Fig. 3(a). The analysis showed that range of AI values varies from 0.5–1.47 over the mentioned period; with the presence of high values (> 1) during pre-monsoon. Data analysis of MODIS Aqua AOD during the same period of observations, also shows a similar trend with peak in pre-monsoon (Fig. 3(b)). The data for Jun–August are missing due to persistent cloudiness. Although mean monthly variations of AOD shows a gradual enhancement of aerosol loading, AI shows sudden peaks during pre-monsoon. This could be due to long range transport of dust, which is observed frequently during pre-monsoon. In addition to high concentration, high altitude aerosol layers are also a significant factor in the high AI values during pre-monsoon. This UV absorbing dust aerosols can be uplifted up to ~500 hPa depending on the convective activity and meteorological conditions (Carlson and Prospero, 1972; Nickling, 1978). Over Tibetan plateau dust layer appear frequently between 4–7 km above mean sea level [msl] (Huang *et al.*, 2007) while Gharai *et al.* (2013) reported vertical extent of dust aerosol over north India is about 6 km during pre-monsoon, 2010. The low AI values during winter and post-monsoon possibly suggest that the aerosols are confined to the near surface because of the presence of shallow boundary layer as well as incidence of long range transport of absorbing aerosols are very less.

To understand about the vertical extent of aerosol, vertical profiles of extinction coefficient (km^{-1}) and PDR obtained from CALIPSO have been analysed. The PDR values indicate the sphericity of aerosols with increasing values pointing towards the degree of irregularity in shape of particles. The values between 0.2–0.31 are generally assumed to be irregularly shaped dust aerosols (Huang *et al.*, 2007) and PDR values below 0.1 are considered as smoke aerosols or aerosols due to anthropogenic origin (Teshce *et al.*, 2009).

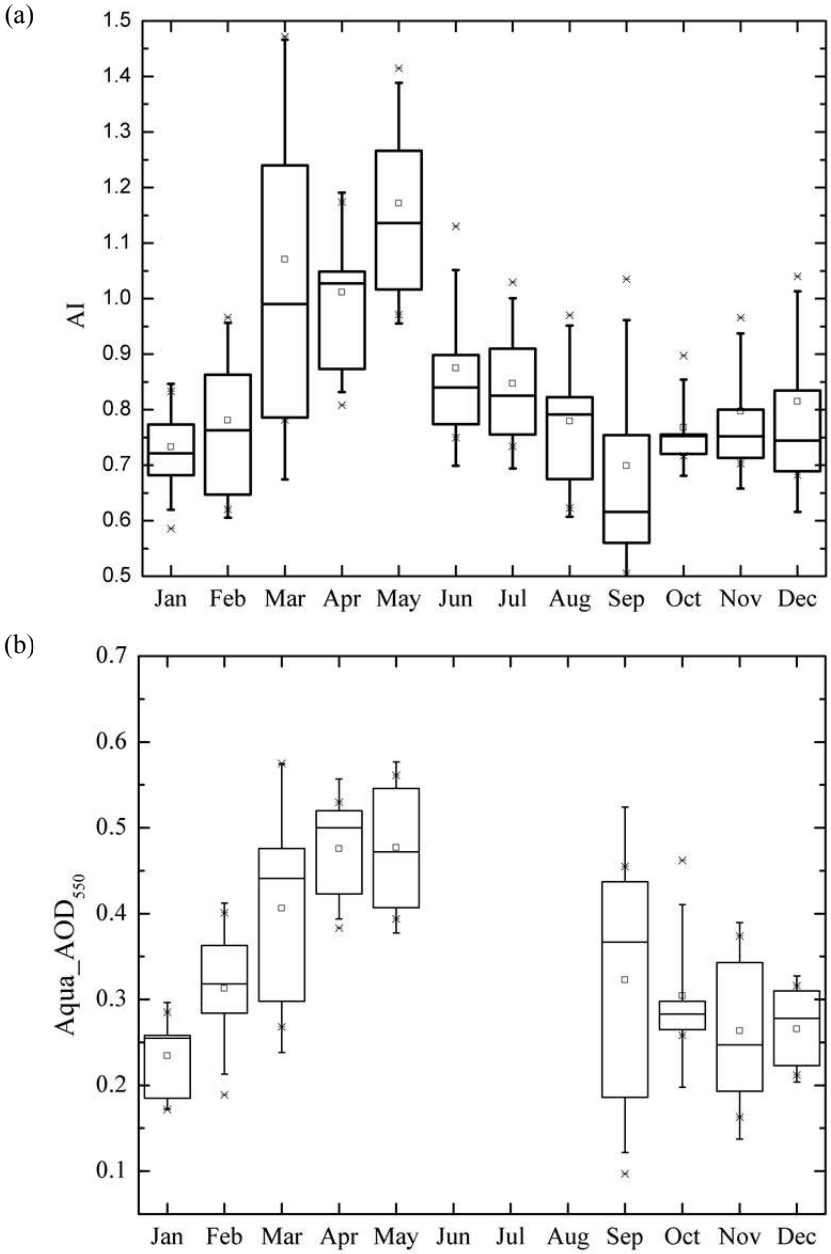

Fig. 3. The box plot monthly mean variation of OMI derived Aerosol Index from 2006–2012.

Kaskaoutis *et al.* (2012) reported high PDR values varying between 0.2–0.5, indicate the presence of dust with nonspherical particles for two dust events occurred at Sahara desert and the eastern Mediterranean. CALIPSO observations profiles are shown in Fig. 4, wherein left and right panel represents pre-monsoon and winter respectively. The extinction profiles represent the averaged values of extinction coefficients (km^{-1}) from the available CALIPSO night tracks during each season and the horizontal bar represents ± 1σ; while the PDR profile represents the number density of aerosol particles. The analysis shows that, the winter season is characterized by high mean extinction values (0.34 km^{-1}) within 1 km, and it decrease with altitude, the PDR profile reveals that ~70% of the particles are within 2 km. This indicates that during winter season majority of the aerosol particles are confined within 2 km from the surface, which may be one of the reason for undetection of UV absorbing aerosol particles by OMI sensor. On the contrary, pre-monsoon profile is characterized by almost constant extinction coefficient with values ranging between 0.1–0.2 km^{-1} and particles throughout the vertical profile (~6 km). It can also be observed that there is a shift in the sphericity of aerosol particles as the season shifts from winter to pre-monsoon. About 70% of the particles during winter have PDR values less than 0.1, while pre-monsoon is characterized by only 25% of the total number of backscattering particles. Increase in PDR values during pre-monsoon indicates the presence of irregularly shaped particles, most probably dust. The variations in the PDR (Fig. 4 bottom panel) are due to the detection noise and

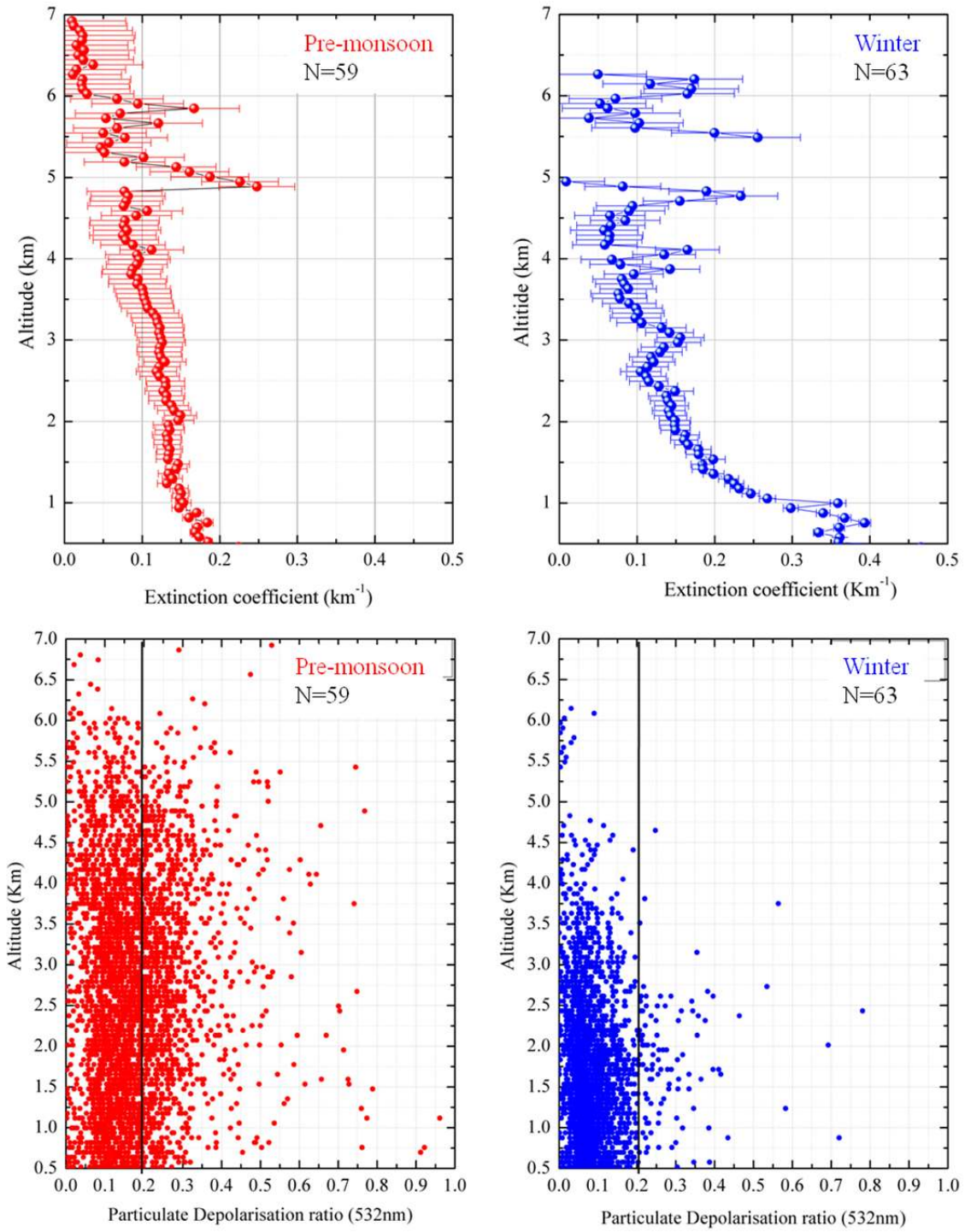

Fig. 4. CALIPSO derived profiles of extinction coefficient (km^{-1}) and Particulate Depolarization Ratio at 532 nm observed during pre-monsoon (Left panel) and winter (Right panel).

natural variability of the dust layer. Although over the study location, CALIPSO derived extinction profiles are limited beyond 6 km height during pre-monsoon, a sharp high aerosol extinction is observed just below 5 km height. Since in this study, we do not have the concurrent vertical profile of meteorological parameters and also non availability of information on contribution of BC to the layer extinction for each profile, it is difficult to explain the actual cause of high extinction observed just below 5 km height above ground level. However Babu *et al.* (2011), found a sharp thin layer of high BC concentration (12 μg m^{-3}) in the altitude region from 4.4–4.8 km during a high altitude balloon experiment with Aethalometer (AE-42, Magee Scientific, USA), which probably associated with high altitude aircraft emission. The above mentioned experimentation was conducted over Hyderabad during pre-monsoon of 2010.

CLUSTER MEAN TRAJECTORY ANALYSIS

The backward trajectories ending at the study site, Hyderabad are investigated over the period 2010–2012 at two levels, 1000 m and 3000 m above ground level (AGL). To investigate the pollutant source regions we separated the trajectories into 4 clusters based on their pathway, namely North–East (N–E), North–West (N–W), South–East (S–E), South–West (S–W). The main criterion of trajectory clustering is to minimize the variability among trajectories and maximize variability among clusters. Cluster mean trajectories of air mass at 3000 m AGL and their percentage contribution to the total calculated for each season over the study period are shown in Fig. 5. Figure shows that majority of the air mass trajectories originating from NW and NE direction of the study site are respectively during post-monsoon (~70%) and winter (~65%). Analysis of trajectories at 1000 m AGL (not shown here) during winter (relatively lower ABL) also suggest that majority air mass are originating from the NW (43%) and NE (29%) directions. During these periods, which are generally the post-harvest period for some of the crops agriculture residue burning, are quite common in the NW and NE regions part of India (Sharma *et al.*, 2010). Frequency distribution of AAE suggest that observed high values of AAE near the surface are more during post-monsoon and winter season (Figs. 2(c) and 2(d)), which could be due to the significant advection of biomass burning aerosols towards the study site from NW and NE directions. The majority of the trajectory pathways during pre-monsoon (~68%) are from the western region of the study site, and a very less number of trajectories (~7%) are observed from north-east (NE) region. The air mass, which follows the NW trajectories are passing over the probable dust source regions like Persian Gulf and Thar desert. This indicates that during pre-monsoon, study site is also influenced by the presence of irregularly shaped coarse mode particles like dust aerosols. During south west monsoon as expected, trajectories are passing through Arabian Sea, which bring marine air mass towards the observation site.

CONCLUSIONS

In the present study an attempt has been made to identify aerosol types over an urban location of Hyderabad based on their absorption properties during 2010–2012. Towards this ground and satellite based observation are used, further HYSPLIT back trajectory model is used to identify possible source location. The important outcomes of the study are the following

(I) Irrespective of the seasonal variation, predominant aerosol types are from fossils fuel and local anthropogenic emissions. BC showed a significant diurnal variation, but a relatively less significant seasonal variation.

(II) Biomass/dust aerosols in its pure form are not found during the study period. However the spread of frequency distribution of AAE reveals the possible presence of these aerosols in different seasons in a mixed state with local BC aerosols.

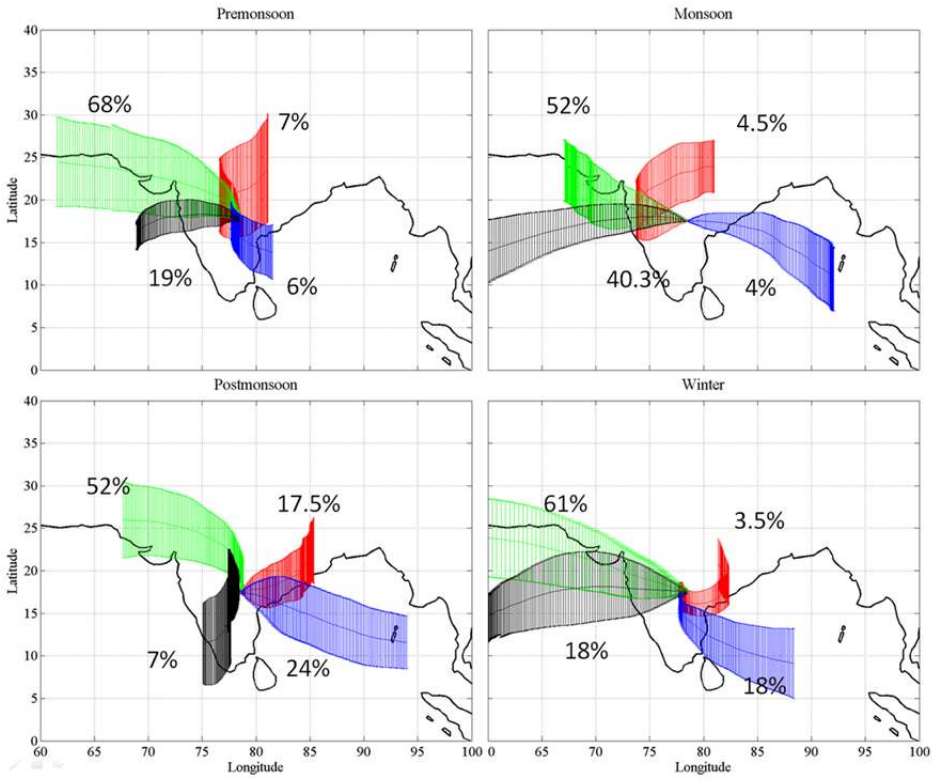

Fig. 5. Cluster mean trajectories of air mass and their percentage contribution to the total, reaching over Hyderabad at an altitude of 3000 m.

(III) The columnar observation of aerosol absorption measurement through AI obtained from OMI sensor reveals that frequency of UV absorbing aerosols are more during pre-monsoon compared to other seasons. In addition to the vertical profile of aerosols, frequent long range transportation of dust aerosols during pre-monsoon is one of the reasons for obtaining high AI during this season.

(IV) Analysis of vertical distribution of aerosols from CALIPSO showed that during winter majority of the aerosols are confined within 2 km from the surface, while in pre-monsoon particles are distributed throughout the profile (~6 km) with extinction coefficient mostly varying between 0.1–0.2 km^{-1}. As the season shift from winter to pre-monsoon a change in sphericity of particle is observed, with particle getting more irregularly shaped during pre-monsoon.

(V) The long range circulation of pollutant pathways reveals that, during pre-monsoon a good proportion of trajectories (~68%) are coming from the western side of study region where, dust prone areas like Thar Desert and Persian Gulf regions are located. During post-monsoon (~70%) and winter (~65%) majority of the trajectory is coming from NW and NE side of Hyderabad, where biomass burning is quite frequent during this period.

ACKNOWLEDGEMENT

The authors gratefully acknowledge Director, NRSC for his encouragement and ISRO-GBP, ARFI project for funding the study. We are also thankful to the entire principal scientist's, NASA GES DISC and Langley centre for providing the satellite data used in study. The authors gratefully acknowledge the NOAA Air Resources Laboratory (ARL) for the provision of the HYSPLIT transport and dispersion model used in this publication. The constructive comments of anonymous reviewers greatly helped to improve the manuscript.

REFERENCES

Alfaro, S.C., Lafon, S., Rajot, J.L., Formenti, P., Gaudichet, A. and Maillé, M. (2004). Iron oxides and light absorption by pure desert dust: An experimental study. *J. Geophys. Res.* 109: D08208, doi: 10.1029/2003 JD004374.

Andreae, M.O. (1995). Climatic Effects of Changing Atmospheric Aerosol Levels. In *World Survey of Climatology*, Chapter 10, Henderson-sellers, A. (Ed.), 16: 347–398.

Andreae, M.O., Jones, C.D. and Cox, P.M. (2005). Strong Present-day aerosol cooling implies a hot future. *Nature* 435: 1187–1190.

Andreae, M.O. and Gelencsér, A. (2006). Black carbon or brown carbon? The nature of light-absorbing carbonaceous aerosols. *Atmos. Chem. Phys.* 6: 3131–3148.

Andrews, E., Ogren, J.A., Bonasoni, P., Marinoni, A., Cuevas, E., Rodríguez, S. and Sheridan, P. (2011). Climatology of aerosol radiative properties in the free troposphere. *Atmos. Res.* 102: 365–393.

Ardanuy, P.E., Kyle, H.L. and Hoyt, D. (1992). Global relationships among the earth's radiation budget, cloudiness, volcanic aerosols and surface temperature. *J. Clim.* 5: 1120–1139.

Arnott, W.P., Hamasha, K., Moosmüller, H., Sheridan, P.J. and Ogren, J.A. (2005). Towards aerosol light-absorption measurements with a 7-wavelength aethalometer: Evaluation with a photoacoustic instrument and 3-wavelength nephelometer. *Aerosol Sci. Technol.* 39: 17–29.

Babu, S.S., Satheesh, S.K. and Moorthy, K.K. (2002). Aerosol radiative forcing due to enhanced black carbon at an urban site in India. *Geophys. Res. Lett.* 29: 1880.

Babu, S.S., Moorthy, K.K., Manchanda, R.K., Sinha, P.R., Satheesh, S.K., Vajja, D.P., Srinivasan, S. and Kumar, V.H.K. (2011). Free tropospheric black carbon aerosol measurements using high altitude balloon: Do BC layers build "their own homes" up in the atmosphere? *Geophys. Res. Lett.* 38: L08803, doi: 10.1029/2011GL 046654.

Beegum, S.N., Moorthy, K.K., Babu, S.S., Satheesh, S.K., Vinoj, V., Badarinath, K.V.S., Safai, P.D., Devara, P.C.S., Singh, S., Vinod, Dumka, U.C. and Pant, P. (2009). Spatial distribution of aerosol black carbon over India during pre-monsoon season. *Atmos. Environ.* 43: 1071–1078.

Bergstrom, R.W., Pilewskie, P., Russell, P.B., Redemann, J., Bond, T.C., Quinn, P.K. and Sierau, B. (2007). Spectral absorption properties of atmospheric aerosols. *Atmos. Chem. Phys.* 7: 5937–5943.

Bergstrom, R.W., Russell, P.B. and Hignett, P. (2002). Wavelength dependence of the absorption of black carbon particles: Predictions and results from the TARFOX experiment and implications for the aerosol single scattering albedo. *J. Atmos. Sci.* 59: 567–577.

Blalock, H.M. (1960). *Social Statistics* (Vol.2). Mc Graw-Hill, New York.

Bond, T.C. and Bergstrom, R.W. (2006). Light absorption by carbonaceous particles: An investigative review. *Aerosol Sci. Technol.* 40: 27–67.

Bond, T.C., Doherty, S.J., Fahey, D.W., Forster, P.M., Berntsen, T., DeAngelo, B.J., Flanner, M.G., Ghan, S., Kärcher, B., Koch, D., Kinne, S., Kondo, Y., Quinn, P.K., Sarofim, M.C., Schultz, M.G., Schulz, M., Venkataraman, C., Zhang, H., Zhang, S., Bellouin, N., Guttikunda, S.K., Hopke, P.K., Jacobson, M.Z., Kaiser, J.W., Klimont, Z., Lohmann, U., Schwarz, J.P., Shindell, D., Storelvmo, T., Warren, S.G. and Zender, C.S. (2013). Bounding the role of black carbon in the climate system: A scientific assessment. *J. Geophys. Res.* 118: 5380–5552.

Carlson, T.N. and Prospero, J.M. (1972). The large-scale movement of Saharan air outbreaks over the northern equatorial Atlantic. *J. Appl. Meteorol.* 11: 283–297.

Charlson, R.J., Langner, J., Rodhe, H., Leovy, C.B. and Warren, S.G. (1991). Perturbation of the northern hemisphere radiative balance by backscattering from anthropogenic sulfate aerosols. *Tellus Ser. A* 43: 152–163.

Clarke, A., McNaughton, C., Kapustin, V., Shinozuka, Y., Howell, S., Dibb, J., Zhou, J., Anderson, B., Brekhovskikh, V., Turner, H. and Pinkerton, M. (2007). Biomass burning and pollution aerosol over North America: Organic components and their influence on spectral optical properties and humidification response. *J. Geophys. Res.* 112: D12S18, doi: 10.1029/2006JD007777.

Collaud Coen, M., Weingartner, E., Apituley, A., Ceburnis, D., Fierz-Schmidhauser, R., Flentje, H., Henzing, J.S., Jennings, S.G., Moerman, M., Petzold, A., Schmid, O. and Baltensperger, U. (2010). Minimizing light absorption measurement artifacts of the aethalometer: Evaluation of five correction algorithms. *Atmos. Meas. Tech.* 3: 457–474.

Patterson, E.M. and McMahon, C.K. (1984). Absorption characteristics of forest fire particulate matter. *Atmos. Environ.* 18: 2541–2551.

De Graaf, M., Stammes, P., Torres, O. and Koelemeijer, R.B.A. (2005). Absorbing aerosol index: Sensitivity Analysis, application to GOME and comparison with TOMS. *J. Geophys. Res.* 110: D01201.

Draxler, R.R. and Rolph, G.D. (2003). HYSPLIT (HYbrid Single-Particle Lagrangian Integrated Trajectory) Model Access via NOAA ARL READY Website (http://www.arl.noaa.gov/ready/hysplit4.html). NOAA Air Resources Laboratory, Silver Spring.

Eck, T.F., Holben, B.N., Sinyuk, A., Pinker, R.T., Goloub, P., Chen, H., Chatenet, B., Li, Z., Singh, R.P., Tripathi, S.N., Reid, J.S., Giles, D.M., Dubovik, O., O'Neill, N.T., Smirnov, A., Wang, P. and Xia, X. (2010). Climatological aspects of the optical properties of fine/coarse mode aerosol mixtures. *J. Geophys. Res.* 115: D19205, doi: 10.1029/2010JD014002.

Fialho, P., Hansen, A.D.A. and Honrath, R.E. (2005). Absorption coefficients by aerosols in remote areas: A new approach to decouple dust and black carbon absorption coefficients using seven-wavelength aethalometer data. *J. Aerosol Sci.* 36: 267–282.

Fuller, K.A., Malm, W.C. and Kreidenweis, S.M. (1999). Effects of mixing on extinction by carbonaceous particles. *J. Geophys. Res.* 104: 15941–15954.

Gadhavi, H. and Jayaraman, A. (2010). Absorbing aerosols: Contribution of biomass burning and implications for radiative forcing. *Ann. Geophys.* 28: 103–111

Ganguly, D., Jayaraman, A. and Gadhavi, H. (2006). Physical and optical properties of aerosols over an urban location in western India: Seasonal variabilities. *J. Geophys. Res.* 111: D24206.

Gharai, B., Jose, S. and Mahalakshmi, D.V. (2013). Monitoring intense dust storms over the Indian region using satellite data – A case study. *Int. J. Remote Sens.* 34: 7038–7048.

Giles, D.M. (2010). Identifying aerosol type/mixture from aerosol absorption properties using AERONET. Eos Trans. AGU 91 (26). Weat. Pac. Geophys. Meet. Suppl.: Abstract A33D–05.

Giles, D.M., Holben, B.N., Eck, T.F., Sinyuk, A., Smirnov, A., Slutsker, I., Dickerson, R.R., Thompson, A.M. and Schafer, J.S. (2012). An analysis of AERONET aerosol absorption properties and classifications representative of aerosol source regions. *J. Geophys. Res.* 117: D17203.

Gyawali, M., Arnott, W.P., Zaveri, R.A., Song, C., Moosmüller, H., Liu, L., Mishchenko, M.I., Chen, L.W.A., Green, M.C., Watson, J.G. and Chow, J.C. (2012). Photoacoustic optical properties at UV, VIS, and near IR wavelengths for laboratory generated and winter time ambient urban aerosols. *Atmos. Chem. Phys.* 12: 2587–2601, doi: 10.5194/acp-12-2587-2012.

Hansen, A.D.A., Rosen, H. and Novakov, T. (1984). The aethalometer—An instrument for the real-time measurement of optical absorption by aerosol particles. *Sci. Total Environ.* 36: 191–196.

Hansen, A.D.A. (1996). *Magee Scientific Aethalometer User'S Guide*. Magee Scientific., Berkeley, California, 56pp.

Hansen, J.E., Sato, M., Lacis, A., Ruedy, R., Tegen, I. and Matthews, E. (1998). Climate forcings in the Industrial era. *Proc. Natl. Acad. Sci. U.S.A.* 95: 12753–12758.

Hansen, J., Sato, M., Ruedy, R., Nazarenko, L., Lacis, A., Schmidt, G.A., Russell, G., Aleinov, I., Bauer, M., Bauer, S., Bell, N., Cairns, B., Canuto, V., Chandler, M., Cheng, Y., Del Genio, A., Faluvegi, G., Fleming, E., Friend, A., Hall, T., Jackman, C., Kelley, M., Kiang, N., Koch, D., Lean, J., Lerner, J., Lo, K., Menon, S., Miller, R., Minnis, P., Novakov, T., Oinas, V., Perlwitz, J., Perlwitz, J., Rind, D., Romanou, A., Shindell, D., Stone, P., Sun, S., Tausnev, N., Thresher, D., Wielicki, B., Wong, T., Yao, M. and Zhang, S. (2005). Efficacy of climate forcings. *J. Geophys. Res.* 110: D18104, doi: 10.1029/2005JD005776.

Haywood, J.M. and Shine, K.P. (1995). The effect of anthropogenic sulfate and soot aerosol on the clear sky planetary radiation budget. *Geophys. Res. Lett.* 22: 603–606.

He, X., Li, C.C., Lau, A.K.H., Deng, Z.Z., Mao, J.T., Wang, M.H. and Liu, X.Y. (2009). An intensive study of aerosol optical properties in Beijing urban area. *Atmos. Chem. Phys.* 9: 8903–8915.

Heintzenberg, J. and Bhardwaja, P.S. (1976). On the accuracy of the backward hemispheric integrating nephelometer. *J. Appl. Meteorol.* 15: 1092–1096.

Herman, J.R., Bhartia, P.K., Torres, O., Hsu, C., Seftor, C. and Celarier, E. (1997). Global distribution of UV-absorbing aerosols from nimbus 7/TOMS data. *J. Geophys. Res.* 102: 16911–16916.

Hoffer, A., Gelencsér, A., Guyon, P., Kiss, G., Schmid, O., Frank, G.P., Artaxo, P. and Andreae, M.O. (2006). Optical properties of humic-like substances (HULIS) in biomass-burning aerosols. *Atmos. Chem. Phys.* 6: 3563–3570.

Huang, J., Minnis, P., Yi, Y., Tang, Q., Wang, X., Hu, Y., Liu, Z., Ayers, K., Trepte, C. and Winker, D. (2007). Summer dust aerosols detected from CALIPSO over the Tibetan Plateau. *Geophys. Res. Lett.* 34: L18805, doi: 10.1029/2007GL029938.

Jacobson, M.Z. (2001). Strong radiative heating due to the mixing state of black carbon in atmospheric aerosols. *Nature* 409: 695–697.

Jacobson, M.Z. (2010). Short-term effects of controlling fossil-fuel soot, biofuel soot and gases and methane on climate, arctic ice, and air pollution health. *J. Geophys. Res.*

115 D14209, doi: 10.1029/2009JD013795.

Kaskaoutis, D.G., Badarinath, K.V.S., Kumar Kharol, S., Rani Sharma, A. and Kambezidis, H.D. (2009). Variations in the aerosol optical properties and types over the tropical urban site of Hyderabad, India. *J. Geophys. Res.* 114: D22204, doi: 10.1029/2009JD012423.

Kaskaoutis, D.G., Prasad, A.K., Kosmopoulos, P.G., Sinha, P.R., Kharol, S.K., Gupta, P., El-Askary, H.M. and Kafatos, M. (2012). Synergistic use of remote sensing and modeling for tracing dust storms in the Mediterranean. *Adv. Meteorol.* 2012: 861026.

Kharol, S.K. and Badarinath, K.V.S. (2006). Impact of biomass burning on aerosol properties over tropical urban region of Hyderabad, India. *Geophys. Res. Lett.* 33: L20801, doi: 10.1029/2006GL026759.

Kirchstetter, T.W., Novakov, T. and Hobbs, P.V. (2004). Evidence that the spectral dependence of light absorption by aerosols is affected by organic carbon. *J. Geophys. Res.* 109: D21208, doi: 10.1029/2004JD004999.

Ma, N., Zhao, C.S., Nowak, A., Müller, T., Pfeifer, S., Cheng, Y.F., Deng, Z.Z., Liu, P.F., Xu, W.Y., Ran, L., Yan, P., Göbel, T., Hallbauer, E., Mildenberger, K., Henning, S., Yu, J., Chen, L.L., Zhou, X.J., Stratmann, F. and Wiedensohler, A. (2011). Aerosol optical properties in the North China Plain during HaChi campaign: An in-situ optical closure study. *Atmos. Chem. Phys.* 11: 5959–5973.

Menon, S., Genio, A.D.D., Koch, D. and Tselioudis, G. (2002). GCM simulations of the aerosol indirect effect: Sensitivity to cloud parameterization and aerosol burden. *J. Atmos. Sci.* 59: 692–713.

Moorthy, K.K., Pillai, P.S. and Babu, S.S. (2003). Influence of changes in the prevailing synoptic conditions on the response of aerosol characteristics to land- and sea-breeze circulations at a coastal station. *Boundary Layer Meteorol.* 108: 145–161.

Moorthy, K.K., Babu, S.S., Satheesh, S.K., Srinivasan, J. and Dutt, C.B.S. (2007). Dust absorption over the "Great Indian Desert" using ground- based and satellite remote sensing. *J. Geophys. Res.* 112: D09206, doi: 10.1029/2006JD007690.

Myhre, G., Myhre, C.E.L., Samset, B.H. and Storelvmo, T. (2013). Aerosols and their relation to global climate and climate sensitivity. *Nature Education Knowledge* 4: 7.

Nair, V.S., Moorthy, K.K., Alappattu, D.P., Kunhikrishnan, P.K., George, S., Nair, P.R., Babu, S.S., Abish, B., Satheesh, S.K., Tripathi, S.N., Niranjan, K., Madhavan, B.L., Srikant, V., Dutt, C.B.S., Badarinath, K.V.S. and Reddy, R.R. (2007). Wintertime aerosol characteristics over the Indo-Gangetic Plain (IGP): Impacts of local boundary layer processes and long-range transport. *J. Geophy. Res*. 112: D13205, doi: 10.1029/2006JD008099.

Nickling, W.G. (1978). Eolian sediment transport during dust storms: Slims River Valley, Yukon Territory. *Can. J. Earth Sci.* 15: 1069–1084.

Niranjan, K., Spandana, B., Anjana Devi, T., Sreekanth, V. and Madhavan, B.L. (2011). Measurements of aerosol intensive properties over Visakhapatnam, India for 2007. *Ann. Geophys*. 29: 973–985.

Penner, J.E., Charlson, R.J., Hales, J.M., Laulainen, N.S., Leifer, R., Novakov, T., Ogren, J., Radke, L.F., Schwartz, S.E. and Travis, L. (1994). Quantifying and minimizing uncertainty of climate forcing by anthropogenic aerosols. *Bull. Am. Meteorol. Soc.* 75: 375–400.

Putaud, J.P., Van Dingenen, R., Alastuey, A., Bauer, H., Birmili, W., Cyrys, J., Flentje, H., Fuzzi, S., Gehrig, R., Hansson, H.C., Harrison, R.M., Herrmann, H., Hitzenberger, R., Hüglin, C., Jones, A.M., Kasper-Giebl, A., Kiss, G., Kousa, A., Kuhlbusch, T.A.J., Löschau, G., Maenhaut, W., Molnar, A., Moreno, T., Pekkanen, J., Perrino, C., Pitz, M., Puxbaum, H., Querol, X., Rodriguez, S., Salma, I., Schwarz, J., Smolik, J., Schneider, J., Spindler, G., ten Brink, H., Tursic, J., Viana, M., Wiedensohler, A. and Raes, F. (2010). A European aerosol phenomenology – 3: Physical and chemical characteristics of particulate matter from 60 rural, urban, and kerbside sites across Europe. *Atmos. Environ.* 44: 1308–1320.

Ram, K., Sarin, M.M. and Tripathi, S.N. (2010). Inter-comparison of thermal and optical methods for determination of atmospheric black carbon and attenuation coefficient from an urban location in northern India. *Atmos. Res.* 97: 335–342.

Ramachandran, S. and Rajesh, T.A. (2007). Black carbon aerosol mass concentrations over Ahmedabad, an urban location in western India: Comparison with urban sites in Asia, Europe, Canada, and the United States. *J. Geophys. Res.* 112: D06211, doi: 10.1029/2006JD007488.

Ramanathan, V. and Carmichael, G. (2008). Global and regional climate changes due to black carbon. *Nat. Geosci.* 1: 221–227.

Rastogi, N. and Sarin, M.M. (2005). Long-term characterization of ionic species in aerosols from urban and high-altitude sites in western India: Role of mineral dust and anthropogenic sources. *Atmos. Environ*. 39: 5541–5554.

Remer, L.A., Tanre, D., Kaufman, Y.J., Levy, R. and Mattoo, S. (2006). Algorithm for Remote Sensing of Tropospheric Aerosol from MODIS: Collection 005. National Aeronautics and Space Administration.

Rosenfeld, D. (1999). TRMM observed first direct evidence of smoke from forest fires inhibiting rainfall. *Geophys. Res. Lett.* 26: 3105–3108.

Rosenfeld, D. (2000). Suppression of rain and snow by urban and industrial air pollution. *Science* 287: 1793–1796.

Sandradewi, J., Prevot, A.S.H., Weingartner, E., Schmidhauser, R., Gysel, M. and Baltensperger, U. (2008). A study of wood burning and traffic aerosols in an Alpine valley using a multi-wavelength Aethalometer. *Atmos. Environ.* 42: 101–112.

Schmid, O., Artaxo, P., Arnott, W.P., Chand, D., Gatti, L.V., Frank, G.P., Hoffer, A., Schnaiter, M. and Andreae, M.O. (2006). Spectral light absorption by ambient aerosols influenced by biomass burning in the Amazon Basin. I: Comparison and field calibration of absorption measurement techniques. *Atmos. Chem. Phys.* 6: 3443–3462.

Schwarz, J.P., Spackman, J.R., Fahey, D.W., Gao, R.S., Lohmann, U., Stier, P., Watts, L.A., Thomson, D.S., Lack, D.A., Pfister, L., Mahoney, M.J., Baumgardner, D., Wilson, J.C. and Reeves, J.M. (2008). Coatings and their enhancement of black carbon light absorption in the tropical atmosphere. *J. Geophys. Res.* 113: D03203, doi: 10.1029/2007JD009042.

Sharma, A.R., Kharol, S.K., Badarinath, K.V.S. and Singh, D. (2010). Impact of agriculture crop residue burning on atmospheric aerosol loading – A study over Punjab State, India. *Ann. Geophys.* 28: 367–379, doi: 10.5194/angeo-28-367-2010.

Silvia, E.D. (2002). Aerosol impacts on visible light extinction in the atmosphere of Mexico City. *Sci. Total Environ.* 287: 213–220.

Sokolik, I.N. and Toon, O.B. (1996). Direct radiative forcing by anthropogenic airborne mineral aerosols. *Nature* 381: 681–683.

Sokolik, I.N. andToon, O.B. (1999). Incorporation of mineralogical composition into models of the radiative properties of mineral aerosol from UV to IR wavelengths. *J. Geophys. Res.* 104: 9423–9444.

Soni, K., Singh, S., Bano, T., Tanwar, R.S., Nath, S. and Arya, B.C. (2010). Variations in single scattering albedo and angstrom absorption exponent during different seasons at Delhi, India. *Atmos. Environ.* 44: 4355–4363.

Stohl, A. (1998). Computation, accuracy and applications of trajectories—A review and bibliography. *Atmos. Environ.* 32: 947–966.

Streets, D.G., Gupta, S., Waldhoff, S.T., Wang, M.Q., Bond, T.C. and Yiyun, B. (2001). Black carbon emissions in China. *Atmos. Environ.* 35: 4281–4296.

Stull, R.B. (1998). *An Introduction to Boundary Layer Meteorology*, Springer, NewYork.

Takemura, T., Nozawa, T., Emori, S., Nakajima, T.Y. and Nakajima, T. (2005). Simulation of climate response to aerosol direct and indirect effects with aerosol transport-radiation model. *J. Geophys. Res.* 110: D02202, doi: 10.1029/2004JD005029.

Tesche, M., Ansmann, A., MÜLler, D., Althausen, D., Mattis, I.N.A., Heese, B., Freudenthaler, V., Wiegner, M., Esselborn, M., Pisani, G. and Knippertz, P. (2009). Vertical profiling of Saharan dust with Raman lidars and airborne HSRL in southern Morocco during SAMUM. *Tellus Ser. B* 61: 144–164.

Torres, O., Bhartia, P.K., Herman, J.R., Ahmad, Z. and Gleason, J. (1998). Derivation of aerosol properties from satellite measurements of backscattered ultraviolet radiation: Theoretical basis. *J. Geophys. Res.* 103: 17099–17110.

Tripathi, S.N., Dey, S., Tare, V. and Satheesh, S.K. (2005). Aerosol black carbon radiative forcing at an industrial city in northern India. *Geophys. Res. Lett.* 32: L08802, doi: 10.1029/2005GL022515.

Valenzuela, A., Olmo, F.J., Lyamani, H., Antón, M., Titos, G., Cazorla, A. and Alados-Arboledas, L. (2015). Aerosol scattering and absorption angström exponents as indicators of dust and dust-free days over Granada (Spain). *Atmos. Res.* 154: 1–13.

Venkataraman, C., Habib, G., Eiguren-Fernandez, A., Miguel, A.H. and Friedlander, S.K. (2005). Residential biofuels in south Asia: Carbonaceous aerosol emissions and climate impacts. *Science* 307: 1454–1456.

Weingartner, E., Saathoff, H., M. Schnaiter, Streit, N., Bitnar, B. and Baltensperger, U. (2003). Absorption of light by soot particles: Determination of the absorption coefficient by means of aethalometers. *J. Aerosol Sci.* 34: 1445–1463.

Winker, D.M., Couch, R.H. and McCormick, M. (1996). An overview of LITE: NASA's lidar in-space technology experiment. *Proc. IEEE* 84: 164–180.

Yan, P. (2006). Study on the Aerosol Optical Properties in the Background Regions in the East Part of China (in Chinese with English Abstract), Ph. D. Thesis, Peking University.

Yang, W., Marshak, A., Várnai, T. and Liu, Z. (2012). Effect of CALIPSO cloud–aerosol discrimination (CAD) confidence levels on observations of aerosol properties near clouds. *Atmos. Res.* 116: 134–141.

Zwally, H.J., Schutz, B., Abdalati, W., Abshire, J., Bentley, C., Brenner, A., Bufton, J., Dezio, J., Hancock, D., Harding, D., Herring, T., Minster, B., Quinn, K., Palm, S., Spinhirne, J. and Thomas, R. (2002). ICESat's laser measurements of polar ice, atmosphere, ocean, and land. *J. Geodyn.* 34: 405–445.

Received for review, October 24, 2014
Revised, April 28, 2015
Accepted, October 20, 2015